Modal analysis of the 0th order nulled phase masks

Wenting Sun (孙文婷), Peng Lv (吕 鹏), Changhe Zhou (周常河)*, Jun Wu (吴 俊), and Shaoqing Wang (王少卿)

Laboratory of Information Optics and Opto-electronic Technology, Shanghai Institute of Optics and Fine Mechanics, Chinese Academy of Sciences, Shanghai 201800, China

**Corresponding author: chazhou@mail.shcnc.ac.cn*

Received January 23, 2013; accepted April 12, 2013; posted online July 3, 2013

A simple modal analysis (MA) method to explain the diffraction process of 0th order nulled phase mask is presented. In MA, multiple reflections of the grating modes at grating interfaces are considered by introducing equivalent Fresnel coefficients. Analytical expressions of the diffraction efficiencies and modal guidelines for the 0th order nulled phase grating design are also presented. The phase mask structure, which comprises a high-index contrast HfO_2 grating and a fused-silica substrate, is optimized using rigorous coupled-wave analysis around the 800-nm wavelength, after which the modal guideline for cancellation of the 0th order in a phase mask is verified. The proposed MA method illustrates the inherent physical mechanism of multiple reflections of the grating modes in the diffraction process, which can help to analyze and design both low-contrast and high-contrast gratings.

OCIS codes: 050.1950, 050.1960, 050.6624.

doi: 10.3788/COL201311.070502.

One important method for fiber Bragg grating (FBG) inscription (writing) is to use 0th order nulled phase masks to fabricate FBGs. This method[1] utilizes the ultraviolet (UV) beam at normal incidence modulated spatially by the phase mask grating made of fused silica, after which the interference of the diffractive 1st and –1st orders exiting from the phase mask forms a periodic pattern, with half the phase mask grating pitch in the photosensitive fiber immediately behind the phase mask. Then, with the use of ultrahigh-peak-power femtosecond (fs) laser radiation for the induction of index change in dielectric materials to produce waveguide structure[2], FBGs are written in standard Ge-doped fiber with pulsed 800-nm laser radiation using a deep-etch silica phase mask[3]. However, previous works[4,5] present evidence that standard fused-silica binary phase masks cannot extinguish the 0th order, where the period is only slightly larger than the exposure wavelength. In addition, the existence of the 0th transmitted order has an unfavorable effect on the formation of a sharp interference pattern with pulsed 800-nm laser when a standard fused-silica binary grating is used. This is because the period of the binary phase mask is around 1 060 nm, which corresponds to the Bragg resonance wavelength[1].

The simplified modal method is an important tool for analyzing low-contrast gratings[6–9], in which the reflection at grating interfaces is neglected. Clausnitzer *et al.*[10] introduced the Fresnel reflection at the interfaces into the simplified modal method using a symmetrical encapsulated grating similar to a standard Fabry-Perot (F-P) cavity. However, only the reflection of one mode is considered in a previous study[10]. For a symmetrical high contrast grating, previous works[11,12] propose an analysis and present an explanation based on a coupled Bloch-mode insight. As far as we know, modal analysis (MA) based on the equivalent F-P interference of dual-mode reflection for an asymmetrical high-contrast grating has yet to be conducted in any study.

In this letter, we propose a new MA method based on the simplified modal method[6] and multi-reflection interference effect of propagating grating modes, thus providing a clear physical image of the diffraction process in a high-contrast phase grating. Analytical expressions of the diffraction efficiencies and modal guidelines for the 0th order nulled phase grating design are provided. Rigorous coupled-wave analysis (RCWA)[13] is used to optimize the phase mask structure. The optimized high-contrast phase grating has an extremely low diffraction efficiency of the 0th order of less than 0.1% under normal incidence, with an 800-nm fs source. The results using RCWA coincide with those from the modal guideline for cancellation of the 0th order in a phase mask. Meanwhile, the effects of incident angle and incident wavelength on the phase mask performance are also considered. Some discussions and conclusions are presented.

Figure 1 shows the schematic of a phase mask structure illuminated under normal incidence at a wavelength λ of 800 nm; it is composed of a substrate with index n_1 (the incidence medium) and a binary grating of thickness h, period Λ, ridge width b, index $n_{\rm r}$, groove width g, and index $n_{\rm g}$. Duty cycle f is defined as the ratio of ridge width b to period Λ. Unlike the standard fused-silica binary phase mask, the phase mask proposed in this letter comprises a higher index contrast grating on a fused-silica substrate. The corresponding refractive indices of the substrate and the groove are 1.45332 and 1.8946 at 800 nm, respectively. The ratio of the grating period to the wavelength should only be between 1 and 2 to ensure only three output diffractive orders, namely, 0th, 1st, and –1st. Moreover, only the 0th and 1st diffraction efficiencies should be considered because the efficiencies of the 1st and –1st diffractive orders are always the same under normal incidence because of their symmetry, i.e., $\theta_1=\theta_{-1}$.

Although the model method is first developed by Collin *et al.*[14,15], it is Botten[16] who first applied it to dielectric gratings. This model method provides a clear

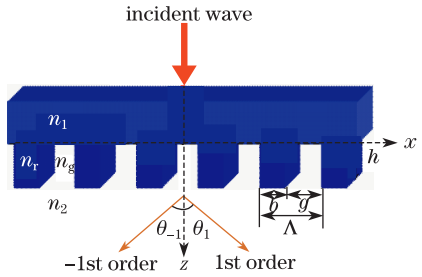

Fig. 1. Schematic of the 0th order nulled phase mask structure consisting of a fused-silica substrate and a higher index contrast binary grating.

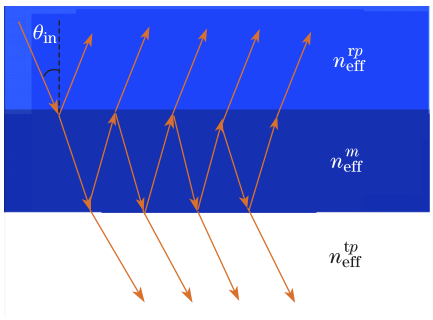

Fig. 2. Schematic illustration of multiple reflections at grating interfaces and the equivalent plane-parallel plate structure of a phase mask grating; θ_{in} is the incident angle, n_{eff}^{m} is the effective index of the mth grating mode, and n_{eff}^{rp} and n_{eff}^{tp} are the effective indices for the pth reflection and transmission order, respectively.

physical insight into the diffraction process by taking the modes of a periodic planar waveguide as the grating modes. When the grating period is comparable to the incident wavelength, only a few propagating grating modes dominate the diffraction process; thus, the diffraction phenomenon becomes comprehensible[17]. As established, the electric field of the mth grating mode inside the grating area has a periodic distribution $u_m(x)$ in the x-direction, propagating along the z-direction with a propagation constant $k_0 n_{eff}^m$. Here, n_{eff}^m is the effective index of the mth grating mode, which can be determined by solving the TE mode dispersion equation[16]

$$\begin{cases} \cos(\beta b)\cos(\gamma g) - \dfrac{1}{2}\dfrac{(\beta^2+\gamma^2)}{\beta\gamma}\sin(\beta b)\sin(\gamma g) \\ \quad = \cos(\alpha_0 \Lambda) \\ \beta = k_0\sqrt{n_r^2 - (n_{eff}^m)^2} \\ \gamma = k_0\sqrt{n_g^2 - (n_{eff}^m)^2}, \alpha_0 = k_0 n_1 \sin\theta_{in} \end{cases}, \quad (1)$$

where k_0 is the wave number in vacuum (k_0=2π/λ), and n_r and n_g are the refractive indices of the grating ridge and groove, respectively. Energy exchange between the incident wave and the grating modes in the x-direction is determined by the overlap integral as[6]

$$\langle E_{yin}(x) \leftrightarrow u_m(x)\rangle = \frac{\left|\int_0^\Lambda E_{yin}(x)u_m(x)\mathrm{d}x\right|^2}{\int_0^\Lambda |E_{yin}(x)|^2\,\mathrm{d}x \int_0^\Lambda |u_m(x)|^2\,\mathrm{d}x}, \quad (2)$$

where $u_m(x)$ and $E_{yin}(x)$ are the electric fields of the mth grating mode and the incident wave, respectively. When the grating period is slightly larger than the incident wavelength, such a grating supports three propagating modes (modes 0, 1, and 2) but two symmetrical modes (modes 0 and 2) can only be excited under normal incidence, which is confirmed by the overlap integral in Eq. (2). Thus, the field at the incident interface of the grating can be expressed as[18]

$$\begin{cases} E_{yin}(x, z=0^+) = a_0 u_0(x)\exp(-\mathrm{j}n_{eff}^0 k_0 z) \\ \quad + a_2 u_2(x)\exp(-\mathrm{j}n_{eff}^2 k_0 z) \\ \quad = a_0^{in} t_{in/0} u_0(x)\exp(-\mathrm{j}n_{eff}^0 k_0 z) \\ \quad + a_2^{in} t_{in/2} u_2(x)\exp(-\mathrm{j}n_{eff}^2 k_0 z) \\ a_m^{in} = \dfrac{\int_0^\Lambda E_{yin}(x)u_m(x)\mathrm{d}x}{\sqrt{\int_0^\Lambda |E_{yin}(x)|^2\,\mathrm{d}x \int_0^\Lambda |u_m(x)|^2\,\mathrm{d}x}} \end{cases}, \quad (3)$$

where a_m is the complex amplitude of the mth grating mode inside the grating area, and $t_{in/m}$ is discussed in detail in the subsequent sections in this letter.

Different from the simplified modal method, wherein the reflection of the grating modes at grating interfaces is neglected due to the low index contrast of the grating[6], the binary grating in this case is a high-index contrast grating, in which the reflections at the grating interfaces play an important role in the diffraction process. As such, the diffraction efficiency functions of the 0th and 1st orders are no longer in a simple sine or cosine form, and the diffraction process is also not as simple as a Mach-Zehnder interferometer[6]. Multiple reflections at grating interfaces in Fig. 2 must be considered to derive the diffraction efficiency expressions. The final diffraction efficiency expressions are similar to the results of the multi-beam interference of a parallel plane plate. The detailed derivation of diffraction efficiency is presented below.

For the mth propagating grating mode, the incident interface can be equivalent to an interface of two mediums with effective indices n_{eff}^{in} and n_{eff}^m. Reflection and transmission coefficients of the mth grating mode at the incident interface can be simply calculated by Fresnel coefficients given by

$$r_{in/m} = \frac{n_{eff}^{in} - n_{eff}^m}{n_{eff}^{in} + n_{eff}^m} = \frac{n_1\cos\theta_{in} - n_{eff}^m}{n_1\cos\theta_{in} + n_{eff}^m}, \quad (4)$$

$$t_{in/m} = \frac{2n_{eff}^{in}}{n_{eff}^{in} + n_{eff}^m} = \frac{2n_1\cos\theta_{in}}{n_1\cos\theta_{in} + n_{eff}^m}, \quad (5)$$

where n_1 is the refractive index of incidence medium. The additional phases of π and 0 at the interfaces are determined by the sign of reflection coefficients. The phase of π means that the beam propagates from an optically thinner medium to an optically denser medium, and phase of 0 is the reverse. Meanwhile, n_{eff}^{in} is defined as the effective index of the incident wave similar with the concept of admittance in thin film optics, equals the perpendicular component of its material refractive index. After multiple reflections and transmissions at the emergent interfaces, the propagating grating modes finally couple out to the reflection and transmission diffractive

orders. Similarly, the effective index of the pth reflection and transmission order (Fig. 2) can be defined as

$$n_{\rm eff}^{rp} = \sqrt{n_1^2 - (k_{xp}/k_0)^2}, \tag{6}$$

$$n_{\rm eff}^{tp} = \sqrt{n_2^2 - (k_{xp}/k_0)^2}, \tag{7}$$

where k_{xp} is determined by the grating equation

$$k_{xp} = k_0 \left[n_1 \sin(\theta_{\rm in}) + p(\lambda/\Lambda) \right]. \tag{8}$$

By introducing effective indices of diffractive orders, reflection and transmission coefficients of the propagating grating modes at the emergent interfaces can be similarly defined by Fresnel coefficients. Here, $r_{m/rp}$ and $t_{m/rp}$ are the reflection and transmission coefficients of the mth grating mode to the pth reflected order at the top interface, respectively. Meanwhile, $r_{m/tp}$ and $t_{m/tp}$ are the reflection and transmission coefficients of the mth grating mode to the pth transmitted order at the bottom interface, respectively.

The reflections of the two modes at the interfaces are independent of each other as the phase mask grating works in a far-off-resonance condition, wherein the coupling between the two propagating modes is extremely weak. Analogous to the multi-beam interference of a plane-parallel plate, complex amplitudes of the mth grating mode contributing to the pth reflection and transmission diffractive order at the emergent interfaces have the forms given below by considering multiple reflections of the grating modes

$$a_m^{rp} = a_m^{\rm in}\Big(r_{{\rm in}/m} + \frac{t_{{\rm in}/m} t_{m/rp} r_{m/tp} {\rm e}^{-2{\rm j}\delta}}{1 - r_{m/tp} r_{m/rp} {\rm e}^{-2{\rm j}\delta}} \Big), \tag{9}$$

$$a_m^{tp} = a_m^{\rm in}\Big(\frac{t_{{\rm in}/m} t_{m/tp} {\rm e}^{-{\rm j}\delta}}{1 - r_{m/tp} r_{m/rp} {\rm e}^{-2{\rm j}\delta}} \Big), \tag{10}$$

where δ=$n_{\rm eff}^m k_0 h$ is the phase at the interface of $z = h$.

Therefore, field distributions of the pth reflection and transmission diffractive orders in x-direction at the emergent interfaces can be written as

$$E_{y{\rm out}}^{rp}(x) = a_0^{rp} u_0(x) + a_2^{rp} u_2(x) \ (z{=}0^-), \tag{11}$$

$$E_{y{\rm out}}^{tp}(x) = a_0^{tp} u_0(x) + a_2^{tp} u_2(x) \ (z{=}h^+). \tag{12}$$

Complex amplitudes of the pth diffractive orders can be derived through the integration of the product of exp $(-{\rm j}k_{xp}x)$ and Eqs. (11) and (12) within a grating period expressed as

$$A_{rp} = \frac{1}{\Lambda} \int_0^{\Lambda} [a_0^{rp} u_0(x) + a_2^{rp} u_2(x)] {\rm e}^{-{\rm j}k_{xp}x} {\rm d}x, \tag{13}$$

$$A_{tp} = \frac{1}{\Lambda} \int_0^{\Lambda} [a_0^{tp} u_0(x) + a_2^{tp} u_2(x)] {\rm e}^{-{\rm j}k_{xp}x} {\rm d}x. \tag{14}$$

The diffraction efficiency of the pth reflection or transmission orders is defined by following the ratio of energy influx given by

$$\eta_p = \frac{n_{\rm eff}^p |A_p|^2}{n_1 \cos(\theta_{\rm in})}, \tag{15}$$

where $n_{\rm eff}^p$ is the effective index of the pth diffractive order defined in Eqs. (6) and (7).

According to Eq. (14), the complex amplitude of the 0th transmitted order can be written as (k_{x0}=0)

$$A_{t0} = \frac{1}{\Lambda} \int_0^{\Lambda} [a_0^{t0} u_0(x) + a_2^{t0} u_2(x)] {\rm d}x. \tag{16}$$

Here, $A_{\rm t0}^0$ and $A_{\rm t0}^2$ are the contributions of mode 0 and mode 2 to the 0th transmitted order, respectively, and are expressed as

$$A_{\rm t0}^0 = \frac{1}{\Lambda} \int_0^{\Lambda} a_0^{\rm t0} u_0(x) {\rm d}x, \tag{17}$$

$$A_{\rm t0}^2 = \frac{1}{\Lambda} \int_0^{\Lambda} a_2^{\rm t0} u_2(x) {\rm d}x. \tag{18}$$

According to the principle of destructive interference, if the conditions below are fulfilled

$$\begin{aligned} &|A_{\rm t0}^0| = |A_{\rm t0}^2| \\ &\Delta\psi = {\rm phase}(A_{\rm t0}^2) - {\rm phase}(A_{\rm t0}^0) \\ &= (2m+1)\pi, \ m = 0, 1, 2 \ ..., \end{aligned} \tag{19}$$

the diffraction efficiency of the 0th transmitted order is 0. This can be used as the guideline for the design of a 0th order nulled phase mask, from which approximate grating parameters can be obtained.

The optimum phase mask structure has a grating period Λ of 1 105, depth h of 466, and duty cycle f of 0.34 using a RCWA algorithm for the TE polarization. Meanwhile, the slight 0th order intensity (<0.1%) and the 1st order intensity are larger than 42.9%, with quite a broad range of structure parameters and grating period ranging from 1 055 to 1 150 nm. Given this condition, the duty cycle from 0.312 to 0.385, and groove depth from 459 to 474 nm are also obtained. In comparison, the diffraction efficiency of the transmitted 0th order is not smaller than 13.4% with optimized parameters for the standard fused-silica phase mask.

Under normal incidence, $\cos(\alpha_0 \Lambda)$ in Eq. (1) is 1. By solving the TE mode dispersion equation, effective indices of the three propagating modes are obtained as follows: $n_{\rm eff}^0$ =1.744, $n_{\rm eff}^1$= 1.264, and $n_{\rm eff}^2$ =0.8 986, with the optimum parameters of Λ=1 105 nm and f=0.34. The normalized mode profiles, which are calculated according to the expression of $u(x)$ in a previous work[16], are shown in Fig. 3. As can be seen, these modes have the same period with the phase mask grating; specifically, mode 0 and mode 2 are symmetrical (even), while mode 1 is asymmetrical (odd).

With the effective indices of the three propagating modes, energy exchanges between modes 0 and 2 and the incident waves at 0.4869 and 0.5032, respectively. In the meantime, the overlap integral of mode 1 with the incident wave is close to 0 according to Eq. (2). Therefore, only the two symmetrical modes can be excited under normal incidence.

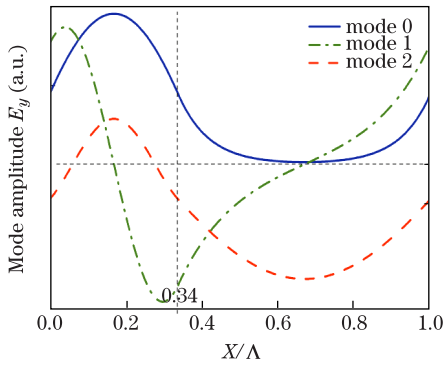

Fig. 3. Normalized mode profiles of the first three modes for the TE polarization (E_y).

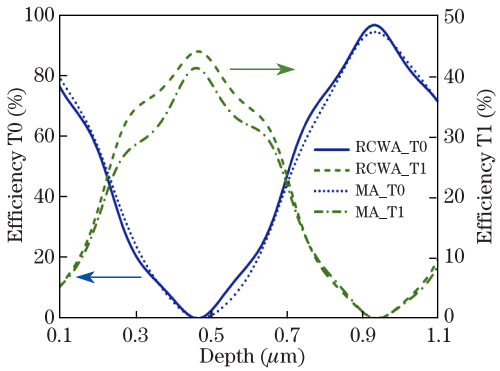

Fig. 4. Diffraction efficiencies of the transmission 0th and 1st diffractive orders versus groove depth calculated by RCWA (solid curves) and the MA method (dashed curves), respectively (Λ=1 105 nm and f=0.34).

After multiple reflections at grating interfaces, the two propagating grating modes finally couple out to reflection and transmission diffractive orders. The contributions of mode 0 and mode 2 to the 0th transmitted order A_{t0}^0 and A_{t0}^2 are defined in Eqs. (17) and (18), respectively. Their amplitudes and phases are shown in Table 1 with the optimum grating depth of 466 nm.

Table 1. Amplitudes and Phases of A_{t0}^0 and A_{t0}^2 and the Phase Difference between A_{t0}^0 and A_{t0}^2

	A_{t0}^2	A_{t0}^0
A_{t0}^m	–0.5890 + 0.0896i	0.5734 – 0.0601i
$\mid A_{t0}^m \mid$	0.5958	0.5765
phase(A_{t0}^m) (rad)	2.9907	–0.1045
$\Delta\psi$ (rad)	3.0952	

Table 1 clearly shows that the amplitude A_{t0}^2 is almost equal to that of A_{t0}^0, and that the phase difference between A_{t0}^0 and A_{t0}^2 is approximate to π. Results in Table 1 are in accordance with the conditions in Eq. (19), verifying the guideline as sufficiently effective to be used in designing 0th order nulled phase masks.

According to Eq. (15), the diffraction efficiencies of the 0th and 1st transmission diffractive orders varying with the grating depth h are calculated (Fig. 4). As can be seen in the figure, the outline of the diffraction efficiency curve of the proposed modal method agrees with that of the RCWA. At the optimum groove depth of 466 nm, the diffraction efficiency of the transmission 0th order is 0.076% and that of the transmission 1st order has a maximum value of 41.1%, showing a slight difference of 2.7% with the maximum efficiency of the transmission 1st order by RCWA. This slight difference between the diffraction efficiencies of RCWA and the proposed MA method can be attributed to the higher order evanescent modes, wherein a fraction of the incident energy is neglected in the MA method. The neglected cross-coupling between the two propagating modes also plays a role in the diffraction efficiencies. Moreover, with the increase of the refractive index contrast between the grating ridge and grating groove, the influence of cross-coupling on the grating diffraction behavior gradually increases. The cross-coupling between the two propagating modes can be obtained by a reflection matrix[11] or scattering matrix[17].

It should be noted that in the simplified MA method, the diffraction efficiencies of the 0th and 1st orders versus the groove depth should obey a standard sine or cosine form. Therefore, multiple reflections at grating interfaces should be a physical cause for explaining the non-sine or non-cosine form (Fig. 4).

A phase mask grating with a certain incident angle range is necessary for practical use. Figure 5(a) shows the diffraction efficiencies of the transmission 0th and 1st orders with varying incident angles at a wavelength of 800 nm using RCWA and the proposed MA method. In the RCWA results, as the incident angle is away from normal incidence, the diffraction efficiency of the 0th order increases gradually, whereas, the 1st order is just the reverse. Within the incident angle range from –9.5° to 15.5°, the diffraction efficiency of the transmission 0th order is always less than 0.1%, whereas, that of the 1st order is more than 40%, making the high-index contrast grating on a fused silica substrate a good 0th order nulled phase mask. The results from the proposed MA method are close to those obtained from RCWA within the incident angle range of –5° to 5°. However, when the incident angle is larger than 5°, the difference between the two results increases rapidly especially for the 0th order. The main cause of the increasing difference is the emergence of the asymmetrical mode 1 due to the deviation from normal incidence. Given that the incident fs laser has a wide wavelength range, the effect of wavelength shift on grating performance would be an important factor to consider. The variations of the diffraction efficiencies of the transmission 0th and 1st orders with the incident wavelength under normal incidence are shown in Fig. 5(b), which clearly shows that the trend of the diffraction efficiency curves from RCWA and the MA method are almost the same. The variation of the difference between the two results is low at just over 81-nm spectral bandwidth. Therefore, the MA method is also useful for analyzing the wideband property of gratings, a topic that shall be discussed in detail in future studies. The difference may be caused by the neglected higher order evanescent modes and the cross-coupling between the two propagating modes mentioned above. As the incident wavelength deviates from the central wavelength of 800 nm, the diffraction efficiency of the 0th order increases gradually. Then, within an 81-nm spectral bandwidth (wavelength ranging from 760 to

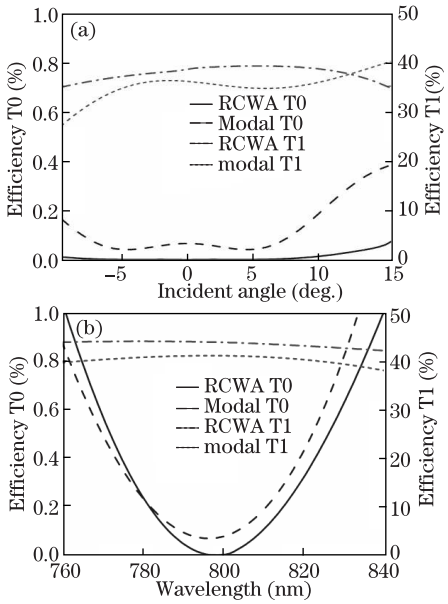

Fig. 5. Diffraction efficiencies of the 0th and 1st diffractive orders as functions of (a) incident angle and (b) incident wavelength using RCWA and the MA method.

841 nm), the diffraction efficiency of the transmission 1st order is always over 42.1%, whereas, that of the transmission 0th order is no more than 1%, thus meeting the requirement of a 0th order nulled phase mask to function as a good wideband beam splitter.

In conclusion, we present a new MA method, which considers multiple reflections of propagating grating modes and provides a clear physical picture of the diffraction process in a phase mask grating. The mechanism of cancellation of the 0th transmitted order is analyzed to provide a modal guideline for the 0th order nulled phase grating design. The optimization design of a 0th order nulled phase mask structure comprising a high-index contrast HfO_2 grating and a fused-silica substrate is also presented. The broad period range of the phase mask grating enables the high peak reflectivity from 1 530 to 1 560 nm of FBGs. The RCWA results verify the modal guideline for cancellation of the 0th order in a phase mask. This view of multiple reflections of the grating modes at grating interfaces reflects inherent physical mechanism and analytical expressions can be used to analyze and design other kinds of gratings in the future[19].

This work was supported by the National Natural Science Foundation of China (Nos. 60878035, 61078050, and 61127013) and the Shanghai Science and Technology Committee (No. 11DZ2290302).

References

1. K. O. Hill, B. Malo, F. Bilodeau, D. C. Johnson, and J. Albert, Appl. Phys. Lett. **62,** 1035 (1993).
2. K. M. Davis, K. Miura, N. Sugimoto, and K. Hirao, Opt. Lett. **21,** 1729 (1996).
3. S. J. Mihailov, C. W. Smelser, P. Lu, R. B. Walker, D. Grobnic, H. Ding, G. Henderson, and J. Unruh, Opt. Lett. **28,** 995 (2003).
4. E. Gamet, A. V. Tishchenko, and O. Parriaux, Appl. Opt. **46,** 6719 (2007).
5. J. Feng, C. Zhou, B. Wang, J. Zheng, W. Jia, H. Cao, and P. Lv, Appl. Opt. **47,** 6638 (2008).
6. T. Clausnitzer, T. Kämpfe, E.-B. Kley, A. Tünnermann, U. Peschel, A. V. Tishchenko, and O. Parriaux, Opt. Express **13,** 10448 (2005).
7. B. Wang, C. Zhou, S. Wang, and J. Feng, Opt. Lett. **32,** 1299 (2007).
8. J. Feng, C. Zhou, J. Zheng, H. Cao, and P. Lv, Appl. Opt. **48,** 5636 (2009).
9. H. Cao, C. Zhou, J. Feng, P. Lu, and J. Ma, Appl. Opt. **49,** 4108 (2010).
10. T. Clausnitzer, T. Kämpfe, E.-B. Kley, A. Tünnermann, A. V. Tishchenko, and O. Parriaux, Opt. Express **16,** 5577 (2008).
11. V. Karagodsky, F. G. Sedgwick, and C. J. Chang-Hasnain, Opt. Express **18,** 16973 (2010).
12. P. Lalanne, J. P. Hugonin, and P. Chavel, J. Lightwave Technol. **24,** 2442 (2006).
13. M. G. Moharam, E. B. Grann, D. A. Pommet, and T. K. Gaylord, J. Opt. Soc. Am. A **12,** 1068 (1995).
14. R. E. Collin, Can. J. Phys. **34,** 398 (1956).
15. S. M. Rytov, Sov. Phys. JETP **2,** 466 (1956).
16. I. C. Botten, M. S. Craig, R. C. McPhedran, J. L. Adams, and J. R. Andrewartha, Opt. Acta **28,** 413 (1981).
17. A. V. Tishchenko, Opt. Quantum Electron. **37,** 309 (2005).
18. J. Zheng, C. Zhou, B. Wang, and J. Feng, J. Opt. Soc. Am. A **25,** 1075 (2008).
19. W. Cao, J. Ma, and C. Zhou, Chin. Opt. Lett. **10,** 112301 (2012).